Journal of Materials Chemistry

Cite this: J. Mater. Chem., 2012, 22, 16209

www.rsc.org/materials

COMMUNICATION

Perpendicularly aligned carbon nanotube/olefin composite films for the preparation of graphene nanomaterials†

Sanqing Huang,[a] Huijuan Lin,[a] Longbin Qiu,[a] Lingli Zhang,[a] Zhenbo Cai,[a] Tao Chen,[a] Zhibing Yang,[a] Shihe Yang[b] and Huisheng Peng*[a]

Received 8th March 2012, Accepted 26th June 2012
DOI: 10.1039/c2jm33009a

There remains a common and critical challenge in the preparation of carbon nanotube (CNT) composite materials, *i.e.*, random dispersion of CNTs in the second phase. Here we have reported a general method to prepare perpendicularly aligned CNT/olefin composite films through a conventional slicing technique. The thickness of a composite film can be accurately controlled from about fifty nanometers to fifty micrometers, and the diameter and density of CNTs may be varied in a wide range as required. In particular, due to the generated defect at the end during the slicing process, the separated CNTs from the composite film have been easily unzipped to produce graphenes in the forms of nanoribbons and nanosheets with a yield of almost 100% under ultrasonic treatment.

In order to improve the practical application, carbon nanotubes (CNTs) have been widely studied to form bulk composite materials.[1–5] Two main methods have been extensively developed to prepare CNT composites, *i.e.*, solution blending and melt blending. Solution blending represents the most common approach in producing CNT composites.[6,7] It mainly includes three steps: dispersion of CNTs in suitable solvents, mixture with the second phase, and fabrication of composites by coating, casting, or precipitation. However, it is difficult to disperse CNTs in solvents by simple stirring. Therefore, high-power ultrasonication had often been used to make metastable suspensions of CNTs in solvents, but the high-power ultrasonication would reduce the aspect ratio of CNTs, which was important to the composite properties.[8] For the melting blending method, high temperature and high shear forces were used to disperse CNTs in the second phase.[9,10] However, compared with solution blending, melt blending is generally less effective at dispersing CNTs and is limited to lower concentrations due to high viscosities at higher CNT loadings. In addition, there remains a common and critical challenge to both methods, *i.e.*, random dispersion of CNTs in the composite material. Therefore, it remains challenging to control the structure and improve the physical properties of the resulting composite materials, which has largely hindered their applications in many fields.

In order to solve the above problem, various modifications, such as the use of an external field, mechanical stretching, spin-casting, melt fiber spinning, and electrospinning, had been investigated.[5] However, the alignment of CNTs still needs to be improved. Recently, aligned CNT materials in the forms of array, film, and fiber have been used as templates to prepare composite materials in which the aligned structure of CNTs could be well maintained.[11–13] In the case of composite films, CNTs were typically horizontally aligned in the second phase.[4]

On the other hand, graphene nanomaterials have attracted increasing attention in recent years due to the novel mechanical and electronic properties.[14–16] A wide variety of approaches were reported for the preparation of graphene nanomaterials, *e.g.*, unzipping CNTs to produce graphene nanoribbons by ultrasonic treatment.[17–19] However, the yield was typically low, *e.g.*, 2%.[18] Although the yield can be greatly improved through an oxidative process, the oxidation may also destroy CNTs.[14]

Herein, we have developed a general method to prepare perpendicularly aligned CNT/olefin composite films in which CNTs were penetrated through the film at a large scale by a conventional slicing technique. Specifically, olefin was firstly infiltrated into a pure CNT array to produce the composite array which could be cut into composite films with accurately tunable thicknesses, typically from about fifty nanometers to fifty micrometers. The CNTs were then separated from the composite film and unzipped to form graphene nanomaterials after an ultrasonic treatment (Fig. 1). Due to the generated defect at the end of CNTs during the slicing process, they can be easily unzipped from one end to the other with a yield of almost 100% without the use of oxidation.

Experimental section

Carbon nanotube (CNT) arrays were synthesized in a tube furnace by a chemical vapor deposition process.[13] The catalyst was first prepared by successive deposition of Al_2O_3 (thickness of 8–15 nm) and Fe (thickness of 0.8–1.2 nm) films on the modified Si wafer with a thin SiO_2 layer at the top (thickness of 1 μm). Typically, C_2H_4 was used as the carbon source, and a mixture of H_2 and Ar gases was used as the carrier gas. The flow rates of C_2H_4, H_2 and Ar were 70–120,

[a]State Key Laboratory of Molecular Engineering of Polymers, Department of Macromolecular Science, and Laboratory of Advanced Materials, Fudan University, Shanghai 200438, China. E-mail: penghs@fudan.edu.cn
[b]Department of Chemistry, Institute of Nano Science and Technology, The Hong Kong University of Science and Technology, Clear Water Bay, Kowloon, Hong Kong, China

† Electronic supplementary information (ESI) available. See DOI: 10.1039/c2jm33009a

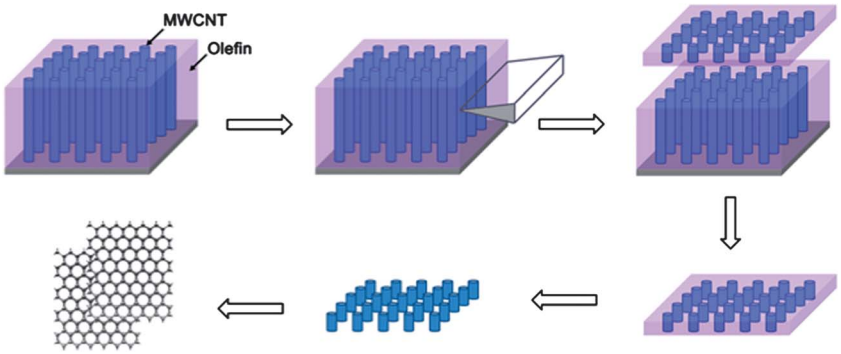

Fig. 1 Schematic illustration of the fabrication of graphene nanomaterials.

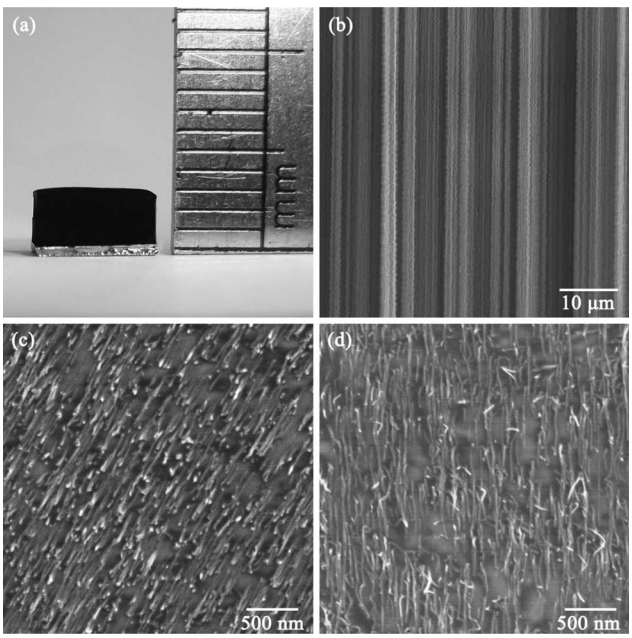

Fig. 2 (a) Photograph of a CNT array. (b) Scanning electron microscopy (SEM) image of (a), side view. (c) SEM image of a CNT/olefin composite film, top view. (d) SEM image of a CNT/olefin composite film, side view.

25–35, 400–500 sccm, respectively. The growth occurred at a temperature between 740 and 790 °C in 40–60 min.

CNT arrays were synthesized by a chemical vapor deposition process which had been previously described.[13] The arrays were first immersed in liquid olefin at 100 °C for 24 h, followed by cooling to room temperature to produce solid CNT/olefin composite arrays. The composite films were prepared by a conventional slicing technique. The CNT/olefin composite films were then heated at 300 °C in vacuum for 24 h and at 900 °C in a mixture of H_2 and Ar gas for 0.5–2 h. Finally, the composite films were immersed in ethanol or dimethyl formamide, followed by ultrasonic treatment for 3–24 h with a frequency of 59 Hz and power of 180 W. The structures were characterized by scanning electron microscopy (SEM) (Hitachi FE-SEM S-4800, operated at 1 kV), transmission electron microscopy (TEM) (JEOL JEM-2100F, operated at 200 kV), and atomic force microscopy (AFM) (SHIMADZU SPM-9500J3). The optical transmittances were measured by UV-vis spectroscopy at a wavelength range of 300 nm to 800 nm (UV-3150, Shimadz). The electrical resistance of the composite film under bending was monitored by an Agilent 34401A digital multimeter. Raman measurements were made on a Renishaw inVia Reflex with an excitation wavelength of 514.5 nm and a laser power of 20 mW.

Results and discussion

The CNTs were perpendicularly grown from the silicon substrate. Fig. 2a shows scanning electron microscopy (SEM) images of a representative CNT array with a height of ~3 mm. Fig. 2b further shows that the CNTs are highly aligned in the array. The height of the CNT arrays may be controlled from about fifty micrometers to four millimeters mainly by varying the growth time, while the diameter of CNTs was mainly controlled from about 8 to 20 nm by varying the thickness of catalyst used and growth temperature (Fig. 3).[20,21] Accordingly, they exhibited increasing wall numbers from 2 to 10.

The CNT arrays were then filled with olefin to produce CNT/olefin composite arrays by dipping pure CNT arrays into liquated olefin at 100 °C, followed by solidification of the olefin. Perpendicularly aligned CNT/olefin composite films were then prepared by slicing the composite array in a direction normal to the CNT length. Fig. 2c and d represent typical SEM images of a CNT/olefin composite film from top and side views, respectively. Obviously, the CNTs maintain the originally aligned state after the infiltration of olefin and formation of the composite film. The CNT densities of as-synthesized arrays ranged from 10^{10} to 10^{11} cm^{-2}, and they can be further improved

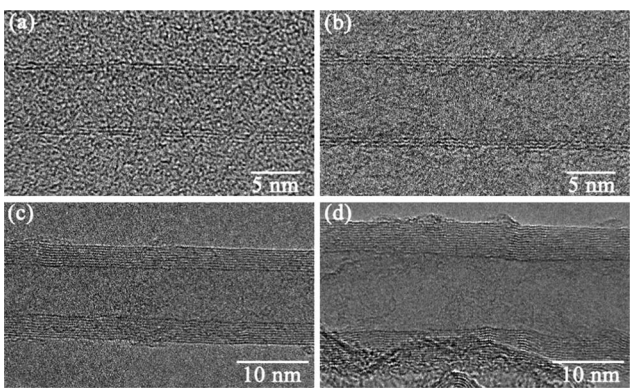

Fig. 3 High-resolution transmission electron microscopy (TEM) images of CNTs with different diameters. (a) 8 nm; (b) 10 nm; (c) 13 nm; (d) 20 nm.

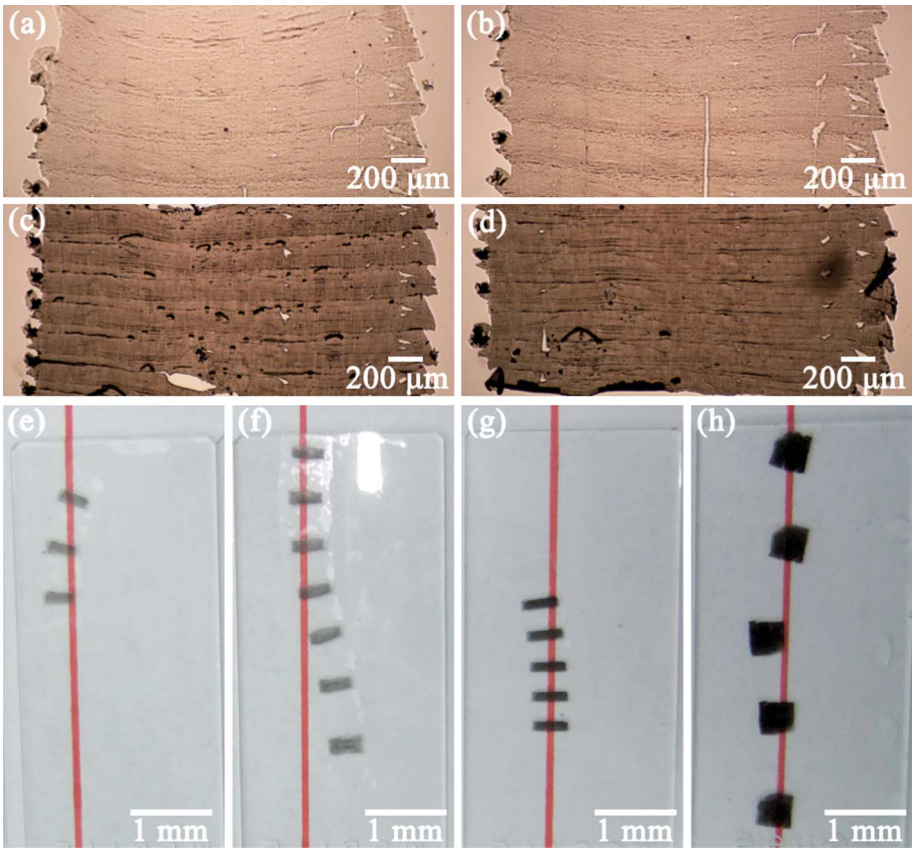

Fig. 4 Optical micrographs and photographs of the CNT/olefin composite film with increasing thickness (δ) from 50 nm to 10 μm. (a) δ = 50 nm; (b) δ = 100 nm; (c) δ = 500 nm; (d and e) δ = 1 μm; (f) δ = 2 μm; (g) δ = 5 μm; (h) δ = 10 μm.

to 10^{12} cm^{-2} by pressing the as-synthesized arrays from one or both sides. The arrays were not observed to shrink after the incorporation of olefin, so the CNT density in the composite array should remain the same as that of the original pure CNT array. In other words, the CNT density of the composite film can be tuned by choosing the pure array with the desired CNT density. A CNT density of 10^{11} cm^{-2} was mainly used in the following discussion. Fig. 4 further shows photographs of composite films with increasing thickness from 50 nm to 10 μm, which were accurately controlled by using an ultramicrotome and a microtome during the preparation. These composite films could be optically transparent with thicknesses of less than 2 μm. The transmittance was further quantitatively measured from 300 nm to 800 nm in wavelength by UV-vis spectroscopy. Fig. S1† shows transmittances above 85% for a composite film with thickness of 100 nm.

Fig. 5 shows typical SEM images of the cross-section of two composite films. Obviously, these composite films are uniform in thickness. As CNTs were perpendicularly aligned and penetrated through the composite film, the length of CNTs was close to the film thicknesses. The composite films were highly flexible and mechanically stable. For instance, the electrical resistances between the top and bottom surfaces of a composite film were monitored under bending, and they remained almost unchanged when it was bent with a different radius (Fig. S2†). After bending for more than 500 cycles, the resistance only varied by less than 4%. Typically, the electrical conductivities in the perpendicular direction of these composite films were calculated on the level of 10^3 S cm^{-1}.

Pure CNTs were separated after the CNT/olefin composite films were heated at 300 °C in vacuum to remove the olefin, followed by calcination at 900 °C in a mixture of Ar and H_2 gases and solvent treatment with ethanol. The resulting materials were carefully investigated by transmission electron microscopy (TEM) and atomic force microscopy (AFM). Fig. 6a and b show typical high-resolution TEM images of two intermediate products, *i.e.*, two CNTs are axially unzipped from the end to form nanoribbons. Fig. S3† further shows

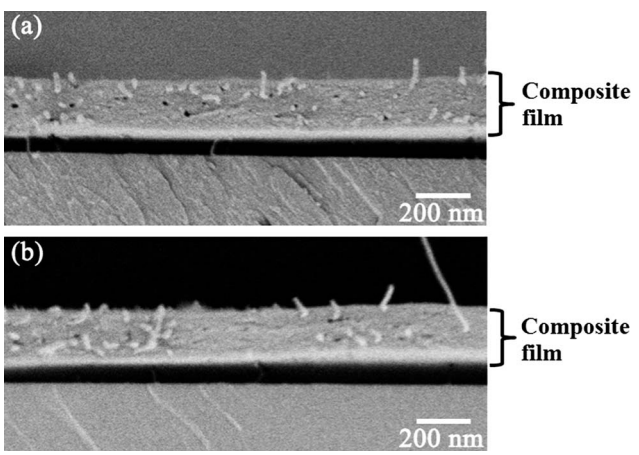

Fig. 5 SEM images of the cross-section of two CNT/olefin composite films which were attached on a glass slide. The film thicknesses are (a) 400 and (b) 350 nm, respectively.

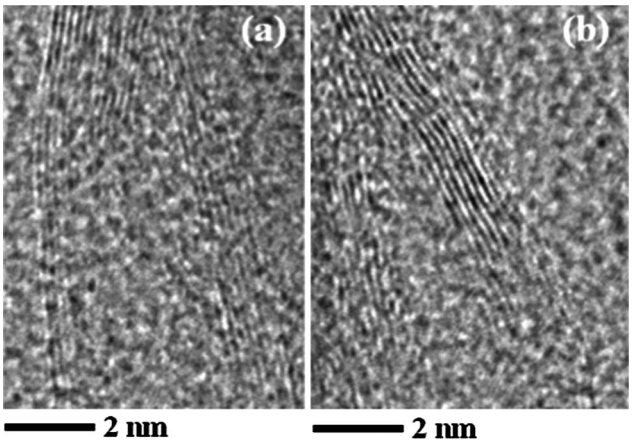

Fig. 6 High-resolution TEM images for the unzipping process of two typical CNTs from one end.

high-resolution TEM images of the final product after sonic treatment of the cut CNTs. The obvious kink structure indicates the production of nanoribbons.[18] As a comparison, the same CNTs without the slicing process were heated and treated by ultrasonication under the same conditions. Fig. S4† showed that the structures of the CNTs were well maintained, and almost no unzipped CNTs were found. Therefore, the produced defects at the CNT end after cutting were mainly responsible for the high unzipping yield, which was further confirmed by AFM. Fig. 7a shows a typical AFM image of the product in Fig. S4.† Obviously, the CNT had not been unzipped. As a contrast, the production of nanosheets was clearly confirmed with different thicknesses from 3.6 to 4.9 nm, which correspond to about 11 to 15 carbon layers, respectively (Fig. 7b).

Fig. 8 shows a typical TEM image of the resulting product after ultrasonic treatment of the CNTs with a length of 60 nm and diameter of 12 nm for 6 h. No CNTs could be found in the product. Additionally, the large area SEM images in Fig. S5† further demonstrate the same result, *i.e.*, no CNTs are observed. The same phenomenon had been observed for the other five different samples. For instance, Fig. S6† shows the product of CNTs with a length of 200 nm and diameter of 8 nm after ultrasonic treatment for 6 h, and almost all the CNTs in the solution were unzipped to produce graphene nanomaterials. This may be explained by the fact that some

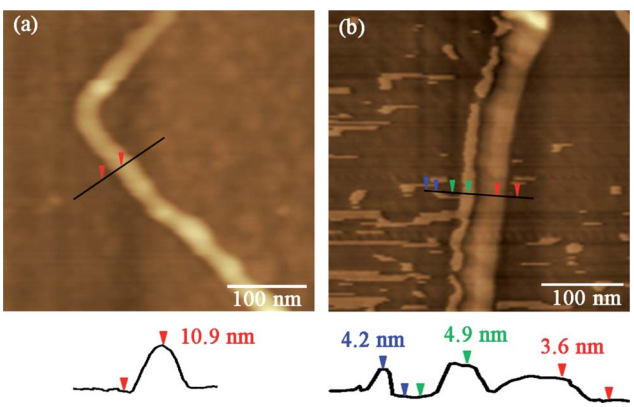

Fig. 7 Atomic force microscopy (AFM) images and height graphs of (a) a treated CNT after heating and (b) the resulting graphene nanosheet after further ultrasonic treatment of the heat-treated CNT.

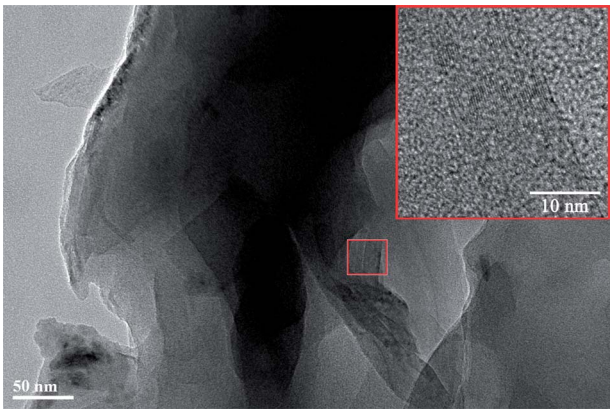

Fig. 8 TEM image of the resulting product after an ultrasonic treatment of heat-treated CNTs (the inset image corresponds to a high magnification).

defects were produced at the end of the CNTs when they were cut during the preparation. This hypothesis was further verified by Raman spectroscopy. Fig. S7† shows typical Raman spectra of the as-synthesized CNTs, CNTs after cutting, and unzipped CNTs. The intensity ratios between D and G bands were 0.47, 0.54, and 0.58, respectively, which indicated the increasing defects in the above three nanomaterials.[22,23] The presence of defects at the end of the CNTs made them unzip more easily under ultrasonication. The resulting nanoribbons or nanosheets could be further coated into films which were also transparent and showed excellent electronic properties. For instance, the transmittance of a nanosheet film with thickness of 40 nm was higher than 80% between 400 and 800 nm in wavelength (Fig. S8†).

It should be noted that pure CNTs were very difficult to directly cut to produce shorter ones as they were very smooth and would slide against each other. As a contrast, here the CNTs were cut into shorter ones due to the stabilization of olefin in the composite. The CNT length may be relatively tuned by varying the thickness of the CNT/olefin composite films. In particular, if a better alignment of CNTs in the composite film and a higher quality of CNTs had been realized, the length of cut CNTs could be accurately controlled as required, and the resulting graphene nanomaterials would show tunable structures and excellent properties. More effort is underway to explore the details.

Conclusions

In summary, a general method has been developed to prepare perpendicularly aligned CNT/olefin composite films through a conventional slicing technique. The film thickness and the CNT diameter and density can be accurately controlled. In particular, the separated CNTs from the composite film were easily unzipped to produce graphenes with a yield of almost 100%, much higher than those of the other fabrication processes based on the CNTs as sources under the same conditions.

Acknowledgements

This work was supported by NSFC (20904006, 91027025), MOST (2011CB932503, 2011DFA51330), MOE (NCET-09-0318), and STCSM (1052nm01600, 11520701400).

Notes and references

1 R. V. Noorden, *Nature*, 2011, **469**, 14.
2 P. M. Ajayan and J. M. Tour, *Nature*, 2007, **447**, 1066.
3 M. Majumder, N. Chopra and B. J. Hinds, *J. Am. Chem. Soc.*, 2005, **127**, 9062.
4 W. Guo, C. Liu, X. Sun, Z. Yang, H. G. Kia and H. Peng, *J. Mater. Chem.*, 2012, **22**, 903.
5 M. Moniruzzamanand and K. I. Winey, *Macromolecules*, 2006, **39**, 5194.
6 S. Barrau, P. Demont, E. Perez, A. Peigney, C. Laurent and C. Lacabanne, *Macromolecules*, 2003, **36**, 9678.
7 M. B. Bryning, D. E. Milkie, M. F. Islam, J. M. Kikkawa and A. G. Yodh, *Appl. Phys. Lett.*, 2005, **87**, 1619091.
8 S. Badaire, P. Poulin, M. Maugey and C. Zakri, *Langmuir*, 2004, **20**, 10367.
9 W.-D. Zhang, L. Shen, I. Y. Phang and T. Liu, *Macromolecules*, 2004, **37**, 256.
10 A. R. Bhattacharyya, T. V. Sreekumar, T. Liu, S. Kumar, L. M. Ericson, R. H. Harge and R. E. Smalley, *Polymer*, 2003, **44**, 2373.
11 H. Peng and X. Sun, *Chem. Commun.*, 2009, 1058.
12 H. Peng, *J. Am. Chem. Soc.*, 2008, **130**, 42.
13 H. Peng, X. Sun, F. Cai, X. Chen, Y. Zhu, G. Liao, D. Chen, Q. Li, Y. Lu, Y. Zhu and Q. Jia, *Nat. Nanotechnol.*, 2009, **4**, 738.
14 D. V. Kosynkin, A. L. Higginbotham, A. Sinitskii, J. R. Lomeda, A. Dimiev, B. K. Price and J. M. Tour, *Nature*, 2009, **458**, 872.
15 X. Chen, L. Li, X. Sun, H. G. Kia and H. Peng, *Nanotechnology*, 2012, **23**, 407640.
16 S. Cho, K. Kikuchi and A. Kawasaki, *Carbon*, 2011, **49**, 3865.
17 A. G. Cano-Marquez, F. J. Rodriguez-Macias, J. Campos-Delgado, C. G. Espinosa-Gonzalez, F. Tristan-Lopez, D. Ramirez-Gonzalez, D. A. Cullen, D. J. Smith, M. Terrones and Y. I. Vega-Cantu, *Nano Lett.*, 2009, **9**, 1527.
18 L. Y. Jiao, X. R. Wang, G. Diankov, H. L. Wang and H. J. Dai, *Nat. Nanotechnol.*, 2010, **5**, 321.
19 A. L. Elias, A. R. Botello-Mendez, D. Meneses-Rodriguez, V. J. Gonzalez, D. Ramirez-Gonzalez, L. Ci, E. Munoz-Sandoval, P. M. Ajayan, H. Terrones and M. Terrones, *Nano Lett.*, 2010, **10**, 366.
20 J. H. Kim, H. S. Jang, K. H. Lee, L. J. Overzet and G. S. Lee, *Carbon*, 2010, **48**, 538.
21 M. H. Ruemmeli, F. Schaeffel, A. Bachmatiuk, D. Adebimpe, G. Trotter, F. Boerrnert, A. Scott, E. Coric, M. Sparing, B. Rellinghaus, P. G. McCormick, G. Cuniberti, M. Knupfer, L. Schultz and B. Buechner, *ACS Nano*, 2010, **4**, 1146.
22 Z.-S. Wu, W. Ren, L. Gao, B. Liu, J. Zhao and H.-M. Cheng, *Nano Res.*, 2010, **3**, 16.
23 P. Kumar, L. S. Panchakarla and C. N. R. Rao, *Nanoscale*, 2011, **3**, 2127.